



## Design and synthesis of several small-size HTLV-I protease inhibitors with different hydrophilicity profiles

Jeffrey-Tri Nguyen, Keiko Kato, Koushi Hidaka, Henri-Obadja Kumada, Tooru Kimura, Yoshiaki Kiso \*

Department of Medicinal Chemistry, Center for Frontier Research in Medicinal Science, Kyoto Pharmaceutical University, Yamashina-ku, Kyoto 607-8412, Japan

### ARTICLE INFO

#### Article history:

Received 20 January 2011

Revised 10 February 2011

Accepted 15 February 2011

Available online 18 February 2011

#### Keywords:

Human T cell lymphotropic virus

HAM/TSP

Adult T cell leukemia

Aspartic protease

Inhibitor

### ABSTRACT

The human T cell leukemia/lymphotropic virus type 1 (HTLV-I) is clinically associated with adult T cell leukemia/lymphoma, HTLV-I associated myelopathy/tropical spastic paraparesis, and a number of other chronic inflammatory diseases. To stop the replication of the virus, we developed highly potent tetrapeptidic HTLV-I protease inhibitors. In a recent X-ray crystallography study, several of our inhibitors could not form co-crystal complexes with the protease due to their high hydrophobicity. In the current study, we designed, synthesized and evaluated the HTLV-I protease inhibition potency of compounds with hydrophilic end-capping moieties with the aim of improving pharmacologic and pharmacokinetic properties.

© 2011 Elsevier Ltd. All rights reserved.

The human T cell leukemia/lymphotropic virus type 1 (HTLV-I) is the first identified human retrovirus<sup>1</sup> and the only known retrovirus to cause human cancer, adult T cell leukemia/lymphoma (ATL).<sup>2</sup> HTLV-I infection may also lead to a chronic progressive myelopathy<sup>3</sup> and several inflammatory diseases as well as opportunistic infections.<sup>4</sup> There is currently no cure for the estimated 20–30 million HTLV-I infected patients<sup>5</sup> living in endemic regions around the world.<sup>6</sup> To develop a cure for HTLV-I infection, we are targeting HTLV-I protease, which is an enzyme responsible for processing precursor proteins to new viral components.<sup>7</sup> HTLV-I protease assumes a C2 symmetry homodimer fold consisting of 125-residue per chain, and grossly resembling the HIV-1 protease. The narrow tunnel-like active site where the precursor protein, substrate or inhibitor is accommodated spans from the symmetrical S<sub>5</sub> to S'<sub>5</sub> subsites (Fig. 1). Tucked between the S<sub>1</sub> and S'<sub>1</sub> subsites, our central P<sub>1</sub> inhibitory unit, a hydroxymethylcarbonyl isostere, is based on the transition state formed during hydrolysis of peptide bonds.

In a recent work, the X-ray diffraction crystallography structures of several of our tetrapeptidic HTLV-I protease inhibitors in complex with a des-(117–125)-[Ile<sup>40</sup>]HTLV-I protease were solved.<sup>8</sup> In the study, only six out of 11 inhibitors formed co-crystals with the protease, because significant precipitation occurred in the preparation mixtures despite extensive screening for other crystallization conditions. The co-crystallized inhibitors were by and large more hydrophilic than those precipitated out of solution. The aim of the current study is to discover small-size

HTLV-I protease inhibitors with different hydrophilicity profiles without jeopardizing the inhibition potency against HTLV-I protease. We selected KNI-10562 (1) as the reference compound, because of its small size and potent inhibition profile against HTLV-I protease (Table 1).

HTLV-I protease has a high degree of specificity for substrates over that of HIV-1 protease<sup>9</sup> and bovine leukemia virus (BLV) protease.<sup>10</sup> Similar to the substrate studies, we reported HTLV-I protease has a high degree of specificity for inhibitors.<sup>7</sup> This means structural requirements at subsites are more stringent for HTLV-I protease binding and inhibition than for HIV-1 protease and BLV protease. The HTLV-I<sup>11</sup> and HIV-1<sup>12</sup> protease inhibition profiles in the current study support this hypothesis, because although the synthesized compounds ranged from low to high HTLV-I protease inhibition (8–93% inhibition at 50 nM), all exhibited potent HIV-1 protease inhibition (72–100% inhibition at 50 nM). Of the subsites, general observations on substrate specificity studies on retroviral aspartic proteases<sup>13</sup> along with our experience with HTLV-I protease inhibitor specificity<sup>14</sup> suggest distant subsites from the catalytic S<sub>1</sub>–S'<sub>1</sub> subsites have lower specificity. This means modifying the two ends of reference inhibitor 1, namely the P'<sub>1</sub>-cap and P<sub>3</sub>-cap moieties, has a lower risk for negatively impacting the HTLV-I protease inhibition potency.

In the current study, using computer-assisted molecular modeling,<sup>15</sup> we designed novel analogues of reference HTLV-I protease inhibitor 1 with different hydrophilic groups to the P'<sub>1</sub>-cap and P<sub>3</sub>-cap moieties. We foresaw the hydrophilic group could either have a direct or water-mediated hydrogen bond interaction with the protease, or otherwise a hydration shell could form at the

\* Corresponding author. Tel.: +81 75 595 4635; fax: +81 75 591 9900.

E-mail address: [kiso@mb.kyoto-phu.ac.jp](mailto:kiso@mb.kyoto-phu.ac.jp) (Y. Kiso).

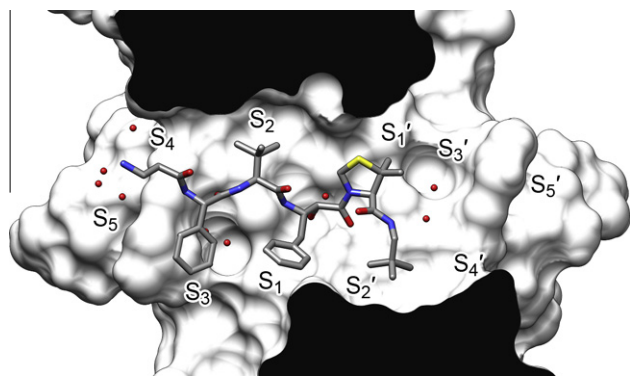


**Figure 1.** Cross-section view with a black slice plane of the active site of HTLV-I protease in complex with inhibitor **5**. Red spheres represent proximal water molecules. Hydrogen bond interactions with the backbone of the inhibitor occur above and below the plane of the page.

modified end of the inhibitor and trap the compound inside the active site. In our computer models, we observed backbone hydrogen bond interactions from the P<sub>1</sub>'-cap to the P<sub>3</sub>-cap moiety were similar in all inhibitors with differences where applicable (Fig. 2). We synthesized the designed compounds (Fig. 3)<sup>16</sup> and screened for greater than 50% HTLV-I protease inhibition at 50 nM. The IC<sub>50</sub> value was determined for any inhibitor passing the screening assay. Lastly, the relative hydrophilicity was evaluated for highly potent inhibitors.

Using reference inhibitor **1** as a starting point, the P<sub>1</sub>'-cap neopentylamine moiety was replaced by more hydrophilic analogues in compounds **2** and **3**. Inhibitor **2** was designed for a hydrogen bond between its distal hydroxyl group and the oxygen atom of Met<sup>37B</sup>. Compared with reference inhibitor **1**, the lower HTLV-I protease inhibition in inhibitor **2** suggests the S<sub>2</sub>' pocket prefers hydrophobic groups. The distal protonated hydrazine nitrogen of the P<sub>1</sub>'-cap *t*-butylhydrazide moiety in inhibitor **3** was designed to form a hydrogen bond with Leu<sup>57B</sup>'s oxygen atom, across from the S<sub>2</sub>' pocket. Inhibitor **3** exhibited slightly lower HTLV-I protease inhibition than reference inhibitor **1**.

At the P<sub>3</sub>-cap region of reference inhibitor **1**, X-ray diffraction crystallography data<sup>8</sup> indicate the nitrogen of the P<sub>3</sub>-cap amide forms a hydrogen bond with the side-chain of Asp<sup>36A</sup>, and the oxygen of the amide has a hydrogen bond interaction with the amide NH of Leu<sup>57A</sup>. Our past study reveals the S<sub>4</sub> subsite can accommodate for several hydrophobic moieties of different length and bulk.<sup>17</sup> Considering the P<sub>3</sub>-cap and P<sub>4</sub> moieties sit at the entrance to the active site, a hydration shell should form with any hydrophilic group introduced in the vicinity. In the current study, the P<sub>3</sub>-cap methyl carbamate moiety in reference inhibitor **1** was first substituted with P<sub>4</sub> glycine as exemplified by inhibitor **4** that was significantly less potent than reference inhibitor **1** (Table 2). Extending the P<sub>4</sub> residue to β-alanine afforded a slightly more potent HTLV-I protease inhibitor (**5**). Further elongation to γ-aminobutyric acid (GABA) led to inhibitor **6** exhibiting lower HTLV-I protease inhibition potency than reference inhibitor **1**. Hence, the potency order from least to most potent for the P<sub>4</sub>-residue is glycine, GABA and β-alanine. Reference inhibitor **7**<sup>17</sup> with a P<sub>3</sub>-cap *n*-butyramide moiety is more structurally similar to P<sub>4</sub> β-alanine inhibitor **5** than P<sub>3</sub>-cap methylcarbamate reference inhibitor **1**. Inhibitor **5** is slightly more potent or equipotent to reference inhibitor **7**, which suggests hydration shell formation is more likely than direct hydrogen bond interaction with the protease.

To explore the effect of two hydrophilic moieties at the P<sub>4</sub> position on HTLV-I protease inhibition, a 1,2,3-diaminopropionic acid residue was introduced in compound **8** to compare with the

**Table 1**

HTLV-I protease inhibition potency of P<sub>1</sub>' analogues

	P <sub>3</sub> -cap	P <sub>3</sub>	P <sub>2</sub>	P <sub>1</sub>	P <sub>1</sub> '	P <sub>1</sub> '-cap
Compounds	R <sup>1</sup>	HTLV-I protease inhibition <sup>11</sup> (IC <sub>50</sub> , nM)	HIV-1 protease inhibition at 50 nM <sup>12</sup> (%)			
<b>1</b>	KNI-10562		7.2 ± 0.6	99		
<b>2</b>	KNI-10608		39.1 ± 5.1	99		
<b>3</b>	KNI-10605		10.4 ± 0.6	99		

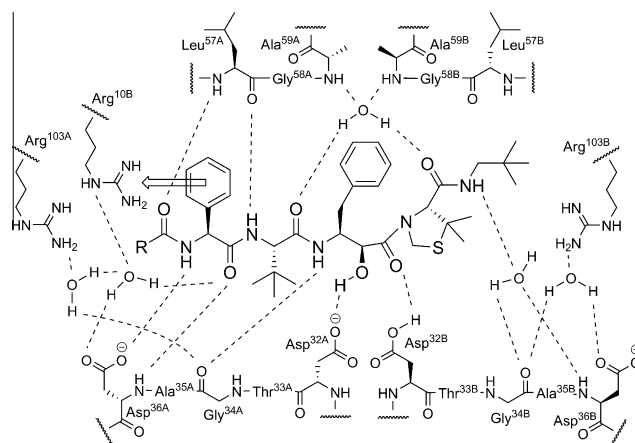


**Figure 2.** A typical hydrogen bond interaction pattern observed in inhibitors **1**, **4–9** and HTLV-I protease. A cation-π interaction is present between the inhibitor's P<sub>3</sub> phenyl group and the protease's Arg<sup>10B</sup> (arrow). For simplicity, intra- and intermolecular hydrogen bond interactions between the two protease chains are not depicted.

possible hydrogen bond interactions found in inhibitors **4** and **5**. Compound **8** exhibited low inhibitory potency against HTLV-I protease. Compound **9** was designed with similar interactions in mind and it too presented with low HTLV-I protease inhibition. Steric hindrance is not likely a problem because the protease can accommodate different hydrophobic bulk in the S<sub>4</sub> subsite.<sup>17,18</sup> It is conceivable hydrogen bond interactions at the S<sub>4</sub> subsite disrupt the favorable interactions elsewhere in the inhibitor. Indeed, our recent X-ray diffraction study on HTLV-I protease inhibitors indicates stronger interactions in the peripheral subsites can pull the tips of the two flaps apart to the extent that two water molecules are bound between the flaps.<sup>8</sup>

Computer-assisted modeling experiments were performed with compounds **4–9** in extended pose to correlate the P<sub>3</sub>-cap/P<sub>4</sub> structure with HTLV-I protease inhibition potency (Fig. 4). The protonated amino group of inhibitor **5**'s P<sub>4</sub> β-alanine is maximally hydrated by three water molecules (Fig. 4D). One of the water molecules mediates a hydrogen bond interaction with Ser<sup>55A</sup>. Another water molecule bridged by a secondary water molecule links inhibitor **5**'s amino group with Asp<sup>36A</sup> to the hydrogen bond network. Thus, inhibitor **5**'s potent inhibition against HTLV-I protease could

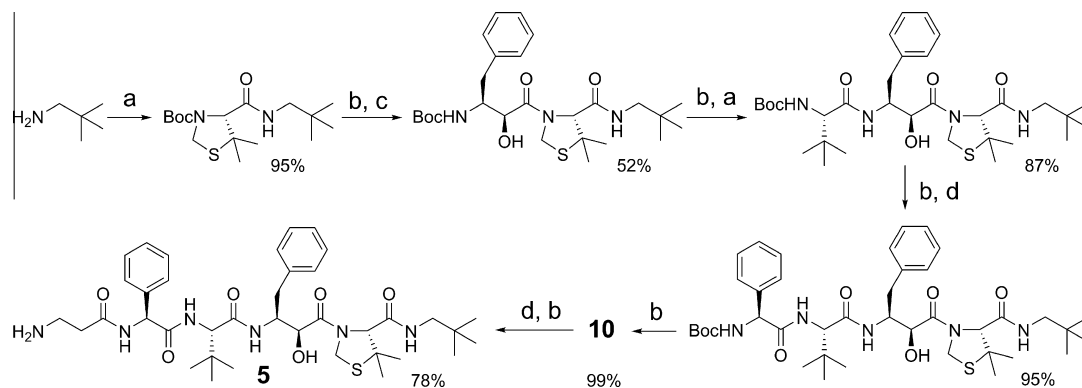


**Figure 3.** A typical synthetic route for exemplified compounds **5** and **10**.<sup>16</sup> Reaction conditions: (a) 1.2 equiv carboxylic acid, 1.3 equiv BOP, DMF, 1.5 equiv Et<sub>3</sub>N, rt, overnight; (b) 4 N HCl in dioxane, rt, 30 min; (c) 1.2 equiv EDC, 1.3 eq HOBt, DMF, rt, 30 min, 1.1 equiv carboxylic acid in DMF, dropwise, then overnight; (d) (pre-activation: 1.2 equiv carboxylic acid, 1.3 equiv CDI, DMF, 1.5 equiv Et<sub>3</sub>N, rt, 1 h), overnight.

**Table 2**  
HTLV-I protease inhibition potency of P<sub>3</sub>-cap and P<sub>4</sub> analogues

Compounds	R <sup>1</sup>	HTLV-I protease inhibition <sup>11</sup> (IC <sub>50</sub> )	HIV-1 protease inhibition at 50 nM <sup>12</sup> (%)	
<b>4</b>	KNI-10856		41.1 ± 11.2 nM	94
<b>5</b>	KNI-10838		5.7 ± 0.4 nM	99
<b>6</b>	KNI-10857		25.4 ± 7.7 nM	99
<b>7</b>	KNI-10635		6.4 ± 1.5 nM	99
<b>8</b>	KNI-10859		8% at 50 nM	72
<b>9</b>	KNI-10858		18% at 50 nM	86
<b>10</b>	KNI-10680		37.0 ± 5.3 nM	>99
<b>11</b>	KNI-10752		31.4 ± 3.8 nM	>99
<b>12</b>	KNI-10767		25.5 ± 4.6 nM	99
<b>13</b>	KNI-10756		44% at 50 nM	92
<b>14</b>	KNI-10753		38% at 50 nM	99
<b>15</b>	KNI-10768		39% at 50 nM	98

be attributed to two water-mediated hydrogen bond interactions. The less potent HTLV-I protease inhibition profiles for compounds **8** (Fig. 4B) and **9** (Fig. 4A) suggest direct hydrogen bond

interactions with Ser<sup>55A</sup> are disfavored, because the interactions pull the protease's two flaps apart. Glycine inhibitor **4** shares a similar water-mediated hydrogen bonding pattern with Asp<sup>36A</sup> and Ser<sup>55A</sup> as β-alanine inhibitor **5** (Fig. 4C). However, the water molecule mediating a hydrogen bond interaction with Ser<sup>55A</sup> also associates with the side-chain of Gln<sup>62A</sup>, thus making the overall interactions at the P<sub>4</sub> position stronger in glycine inhibitor **4** than β-alanine inhibitor **5**. In the case of GABA inhibitor **6**, a hydration shell is present (Fig. 4E). The lack of direct or strong water-mediated hydrogen bond interaction with the protease contributes to inhibitor **6**'s higher inhibition potency than compounds **4**, **8** and **9**. However, the weaker association with the protease at the S<sub>4</sub> subsite renders inhibitor **6** less potent than inhibitor **5**. Taking together, we assume hydrophobic bulk is a minor factor<sup>17,18</sup> and propose HTLV-I protease inhibition potency at the S<sub>4</sub> subsite is determined by a hydrogen bond balance between strong interactions in compounds **4**, **8** and **9** and weak interactions in inhibitor **6**. The more potent inhibitor **5** has well balanced hydrogen bond interactions. However, from the same line of reasoning, reference inhibitor **7** should exhibit low potency because of the absence of hydrogen bond interactions at the P<sub>4</sub> position, yet the hydrophobic compound is quite potent against HTLV-I protease (Fig. 4F). The current study demonstrates P<sub>4</sub> hydrophilic groups, on the other hand, significantly affect protease inhibition from 8% (compound **8**) to 90% (compound **5**) at 50 nM compound concentrations. Hence, we speculate hydrophobic moieties are generally preferred at the P<sub>4</sub> position over hydrophilic moieties, unless there are P<sub>4</sub> hydrogen bond interactions anchoring the inhibitor in the active site without pulling the protease's flaps apart.

In the previously reported X-ray diffraction crystallography study, tetrapeptidic HTLV-I protease inhibitors with a free P<sub>3</sub> amino group formed co-crystals with the mutant protease.<sup>8</sup> Hence, the P<sub>3</sub>-cap truncated analogue of reference inhibitor **1**,<sup>17</sup> namely compound **10**, is expected to also form co-crystals with the protease. It is noteworthy reference inhibitor **10** is less potent than reference inhibitor **1** because of a missing important hydrogen bond interaction with the protease's Leu<sup>57A</sup>. The P<sub>3</sub> amino group forms an important hydrogen bond with the protease's Asp<sup>36A</sup>. Appending a methyl group in inhibitor **11** or an ethyl group in inhibitor **12** seems to successively improve the inhibition profiles. However, the presence of a benzyl moiety as the P<sub>3</sub>-cap moiety in compound **13** is less favored by the protease than ethyl-capped inhibitor **12**. During the synthesis of inhibitors **11** and **12**, the respective disubstituted compounds **14** and **15** were isolated after a nucleophilic substitution reaction. Although the tertiary amino group in compounds **14** and **15**, once protonated to a quaternary salt, can have hydrogen bond interactions with Asp<sup>36A</sup>, the inhibition profiles are

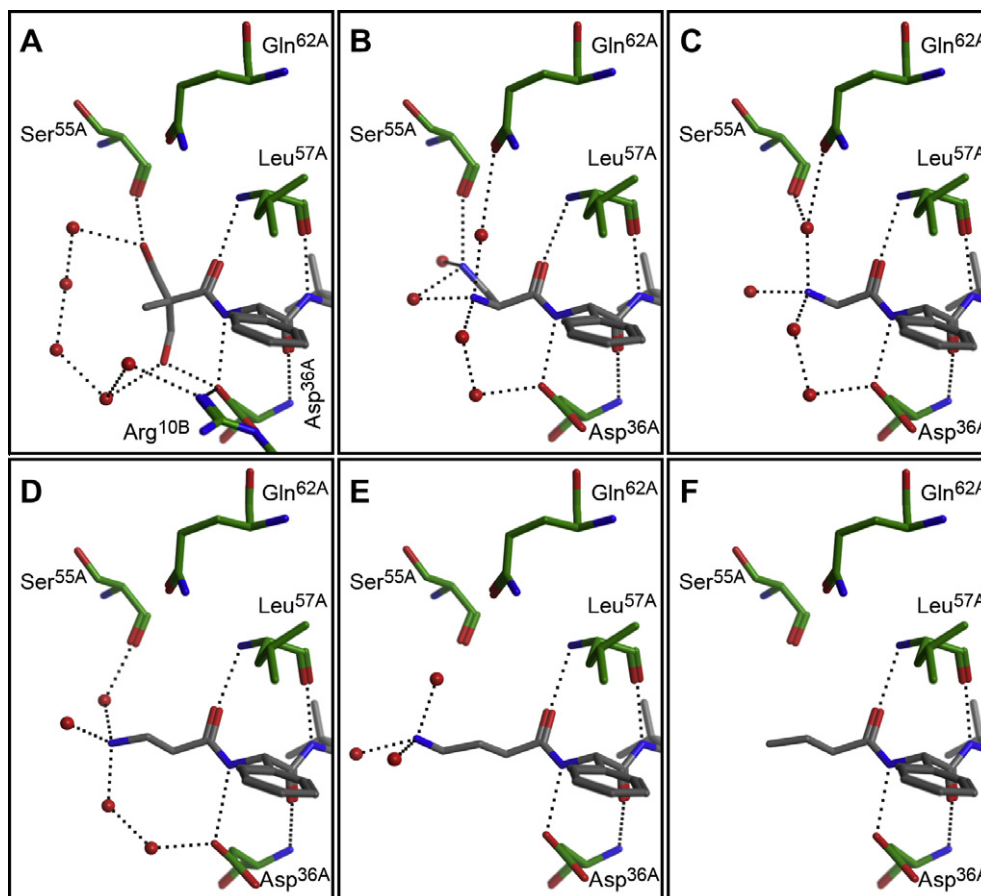


**Figure 4.** Hydrogen bond interactions observed at the  $P_4$  position in the extended pose of compounds (A) **9**, (B) **8**, (C) **4**, (D) **5**, (E) **6** and (F) **7**. For simplicity, only water molecules interacting with the compound at the  $S_4$  subsite are depicted. Water molecules are red spheres, protease residues are green, and the compound is gray.

as expected less potent than their primary and secondary amine analogues (**10–12**). As previously mentioned, the occupancy in the  $S_4$  subsite by a hydrophobic group is a minor determinant of HTLV-I protease inhibition potency<sup>17,18</sup> and the moderate changes in the inhibition profiles of compounds **10–15** (38–62% at 50 nM) support this generalization.

Compounds **1**, **3**, **5** and **7** were selected for relative hydrophilicity profiling based on their high potency against HTLV-I protease with  $IC_{50}$  values less than 15 nM. Their hydrophilicity profiles were estimated using three calculation methods examining their calculated  $\log P$  (log of the octanol/water partition coefficient including implicit hydrogens),<sup>15</sup>  $S \log P$  ( $\log P$  calculation that accounts for acidic protonation state)<sup>19</sup> and  $\log S$  (log of the aqueous solubility [mol/L])<sup>20</sup> values. The relative hydrophilicity for the compounds was experimentally determined by their mobility in an HPLC gradient mixture of acetonitrile and aqueous 0.1% trifluoroacetic acid (Fig. 5). The HPLC chart suggests  $S \log P$  is more accurate than calculated  $\log P$  and  $\log S$  at predicting the relative hydrophilicity order of the compounds—from most to least hydrophilic, compounds **3**, **5**, **1** and **7**. Because of its N-terminal carbamate nitrogen, compound **1** is sufficiently hydrophilic to form co-crystal complexes with HTLV-I protease.<sup>8</sup> In addition to the carbamate group, compound **3** has a  $P'_1$ -cap hydrazide nitrogen that can be protonated under the experimental acidic aqueous conditions to render it more hydrophilic than its reference compound **1**. Similarly the  $P_4$   $\beta$ -alanine amino group in compound **5** is protonated under experimental conditions to make the compound more hydrophilic than its reference compound **7**. As described in our X-ray crystal study,<sup>8</sup> significant

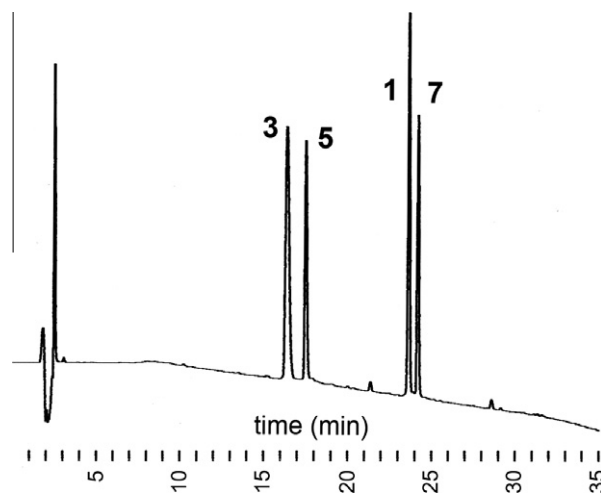


**Figure 5.** HPLC chart of a mixture of pure compounds **1**, **3**, **5** and **7**. In this reverse phase HPLC running with a linear 20–100% gradient of acetonitrile (30 min, 2 min delay) in 0.1% aqueous trifluoroacetic acid, the more hydrophilic compounds have shorter retention time.

precipitation was observed in mixtures of HTLV-I protease and a hydrophobic inhibitor resembling compound **7**, and despite extensive screening for several crystallization conditions, crystals were not formed. That being said, we also expect similar difficulties with hydrophobic compound **7**. On the other hand, several



structurally similar hydrophilic compounds with a P<sub>3</sub> free amino group can form co-crystal complexes with the protease.<sup>8</sup> Hence, we anticipate the formation of co-crystal HTLV-I protease complexes with hydrophilic compounds **3** and **5**. In addition, these compounds with different hydrophilicity properties should also facilitate future pharmaceuticals and drug formulation studies.

From a pharmacokinetic perspective, the hydrophilicity of a compound plays a significant role in its absorption in the gastrointestinal tract, subsequent metabolism in the gut wall and liver, and clearance. One should note the P<sub>3</sub>-cap methylcarbamate group of compound **1** might be degraded in vivo under acid–base conditions to produce less potent inhibitor **10**. Similar problems might arise from compound **3**. Computational pharmacokinetics suggest oral bioavailability is likely for compounds with log *P* values between –0.4 and 5.6.<sup>20</sup> The calculated log *P* values for compounds **1**, **3**, **5** and **10** fall within range (from 3.8 to 5.1) with hydrophobic compound **7** at the borderline (log *P* = 5.7). Being hydrophobic, compound **7** has a higher risk for unwanted binding with untargeted biological substances, such as plasma proteins, that delay and prevent the compound from reaching the target site of action. Conversely, high water solubility compounds have higher renal clearance from the body. However, high renal clearance is not expected in compounds **1**, **3**, **5**, **7** and **10**, because they are not highly hydrophilic. On the other hand, diverse types of metabolic reactions can occur with compounds **3**, **5** and **10** at the respective nitrogen, such as glucuronide formation, that may deactivate and assist in their removal from the body.<sup>21</sup> Nevertheless, the P<sub>1</sub>-cap hydrazide free nitrogen in compound **3** should have relatively lower metabolic reactivity because of steric bulk from the adjacent *t*-butyl group. Overall, in designing our compounds, we looked not only at potent inhibition against HTLV-I protease but also at a series of compounds with a large spread in their hydrophilicity profiles. Now, having established P<sub>1</sub>-cap *t*-butyl hydrazide and P<sub>4</sub> β-alanine moieties increase hydrophilicity without greatly affecting HTLV-I protease inhibition potency, we could evaluate compounds with several P<sub>1</sub>-cap bulky hydrazide groups and various P<sub>3</sub>-cap amido or P<sub>4</sub> β-alanine moieties in future studies to obtain a larger selection of potent HTLV-I protease inhibitors with a wide range of hydrophilicity property.

In the current study, we designed and synthesized HTLV-I protease inhibitors with the aim of retaining high inhibition potency with a good mix of hydrophilicity profiles. We succeeded in identifying inhibitors **1**, **3**, **5** and **7** that have IC<sub>50</sub> values less than 15 nM and an adequate spread in hydrophilicity.

## Acknowledgments

This study was supported in part by the 'Academic Frontier' Project for Private Universities, a matching fund subsidy from the Ministry of Education, Culture, Sports, Science and Technology (MEXT), Japan. We thank Mr. T. Hamada for performing HIV-1 protease inhibition assay.

## Supplementary data

Supplementary data associated with this article can be found, in the online version, at doi:10.1016/j.bmcl.2011.02.066.

## References and notes

- Poiesz, B. J.; Ruscetti, F. W.; Reitz, M. S.; Kalyanaraman, V. S.; Gallo, R. C. *Nature* **1981**, *294*, 268.
- Takatsuki, K. *Retrovirology* **2005**, *2*, 16.
- Jacobson, S. J. *Infect. Dis.* **2002**, *186*, 187.
- Semmes, O. J. *J. Clin. Invest.* **2006**, *116*, 858.
- Nicot, C. *Am. J. Hematol.* **2005**, *78*, 232.
- Proietti, F. A.; Carneiro-Proietti, A. B.; Catalan-Soares, B. C.; Murphy, E. L. *Oncogene* **2005**, *24*, 6058.
- Nguyen, J. T.; Kiso, Y. In *Viral Proteases and Antiviral Protease Inhibitor Therapy: Proteases in Biology and Disease*; Lendeckel, U., Hooper, N. M., Eds.; Springer Science: Dordrecht, 2009. Vol. 8, pp 83–100.
- Satoh, T.; Li, M.; Nguyen, J.-T.; Kiso, Y.; Gustchina, A.; Wlodawer, A. J. *Mol. Biol.* **2010**, *401*, 626.
- Kádas, J.; Weber, I. T.; Bagossi, P.; Miklóssy, G.; Boross, P.; Orozslan, S.; Tözsér, J. *J. Biol. Chem.* **2004**, *279*, 27148.
- Tözsér, J. *Viruses* **2010**, *2*, 147.
- Recombinant L40I mutation HTLV-I protease percent inhibition potency at 50 nM of the test compound was evaluated as single determinations using previously reported procedures.<sup>8</sup> IC<sub>50</sub> values were calculated from the sigmoid plot derived by percent inhibition data at 1, 5, 10, 20, 50 and 100 nM of the test compound, as a single determination at each concentration, using Synergy Software's Kaleidagraph (Supplementary data). The error range for IC<sub>50</sub> values was calculated from the root mean square deviation (RMSD) of the plot, that is, 50% ± RMSD inhibition.
- Recombinant HIV-1 protease percent inhibition potency at 50 nM of the test compound was evaluated as single determinations using previously reported procedures.<sup>22</sup>
- Tözsér, J.; Zahuczky, G.; Bagossi, P.; Copeland, J. M.; Orozslan, S.; Harrison, R. W.; Weber, I. T. *Eur. J. Biochem.* **2000**, *267*, 6287.
- Kimura, T.; Nguyen, J.-T.; Maegawa, H.; Nishiyama, K.; Arii, Y.; Matsui, Y.; Hayashi, Y.; Kiso, Y. *Bioorg. Med. Chem. Lett.* **2007**, *17*, 3276.
- Computer-assisted modeling experiments and chemical property calculations were performed using Molecular Operating Environment 2009.1001 (MOE), and modeled from PDB 3LIN. When studying the involvement of water (Fig. 4), a sphere (10 Å) of water was generated around the compound's amino or hydroxyl groups using MOE's Water-Soak function. The system was energy minimized using the LigX function under MMFF94x force-field: the proximal (8 Å) protease heavy atom residues were tethered while the compound was flexible. Visualization of the subsites (Fig. 1) was assisted by UCSF Chimera 1.4.1.
- The synthesis of reference compounds **1**,<sup>8</sup> **7**<sup>17</sup> and **10**<sup>17</sup> was previously described (Fig. 3). Compounds **1–15** were synthesized by standard solution phase peptide synthesis by which sequential elongation and coupling of an amine to a carboxylic acid was performed in DMF with benzotriazol-1-yl-oxy-tris-(dimethylamino)phosphonium hexafluorophosphate (BOP) or *N,N*-carbonyldiimidazole (CDI) as coupling reagent and Et<sub>3</sub>N as base. Although BOP was favored over CDI for coupling to the P<sub>1</sub>' residue, CDI showed higher coupling reactivity with bulky amines. Peptide coupling to the P<sub>1</sub> residue was accomplished using 1-ethyl-3-(3-dimethylaminopropyl) carbodiimide hydrochloride (EDC) and 1-hydroxybenzotriazole (HOBt) as additive, without a base, to avoid reported side-reactions.<sup>23</sup> Attachment of a Boc protection group to an amino group was achieved with Boc<sub>2</sub>O and Et<sub>3</sub>N in DMF, while the removal of the Boc protection group was achieved with 4 N HCl in dioxane. The hydroxyl group in compounds **2** and **9** was acetyl protected with acetic anhydride in pyridine, and eventually removed by a 50% v/v mixture of 4 N NaOH(aq) and MeOH. The N-terminal cap was appended in DMF and Et<sub>3</sub>N as base by a reaction with methyl chloroformate for compounds **2** and **3**, or with benzylbromide for compound **13**. The nucleophilic substitution reactions in compounds **11**, **12**, **14** and **15** was performed with methyl iodide or ethyl iodide, respectively, to afford a mixture of mono- and disubstituted products. After preparative HPLC purification, all target compounds (**1–15**) were >95% pure by analytical HPLC (Supplementary data). The identities of the compounds were confirmed by TOF MS and ESI-Q MS.
- Zhang, M.; Nguyen, J.-T.; Kumada, H. O.; Kimura, T.; Cheng, M.; Hayashi, Y.; Kiso, Y. *Bioorg. Med. Chem.* **2008**, *16*, 6880.
- Zhang, M.; Nguyen, J.-T.; Kumada, H. O.; Kimura, T.; Cheng, M.; Hayashi, Y.; Kiso, Y. *Bioorg. Med. Chem.* **2008**, *16*, 5795.
- Oprea, T. I.; Davis, A. M.; Teague, S. J.; Leeson, P. D. *J. Chem. Inf. Comput. Sci.* **2001**, *41*, 1308.
- Hou, T. J.; Xia, K.; Zhang, W.; Xu, X. J. *J. Chem. Inf. Comput. Sci.* **2004**, *44*, 266.
- Yoshida, F.; Topliss, J. G. *J. Med. Chem.* **2000**, *43*, 2575.
- Maegawa, H.; Kimura, T.; Arii, Y.; Matsui, Y.; Kasai, S.; Hayashi, Y.; Kiso, Y. *Bioorg. Med. Chem. Lett.* **2004**, *14*, 5925.
- Hayashi, Y.; Kinoshita, Y.; Hidaka, K.; Kiso, A.; Uchibori, H.; Kimura, T.; Kiso, Y. *J. Org. Chem.* **2001**, *66*, 5537.